Journal of Macromolecular Science, Part A
Publication details, including instructions for authors and subscription information:
http://www.informaworld.com/smpp/title~content=t713597274

Degradation Profile of Poly(ε-caprolactone)-the Influence of Macroscopic and Macromolecular Biomaterial Design

Anders Höglund[a]; Minna Hakkarainen[a]; Ann-Christine Albertsson[a]
[a] Department of Fibre and Polymer Technology, School of Chemical Science and Engineering, Royal Institute of Technology, Stockholm, Sweden

To cite this Article Höglund, Anders , Hakkarainen, Minna and Albertsson, Ann-Christine(2007) 'Degradation Profile of Poly(ε-caprolactone)-the Influence of Macroscopic and Macromolecular Biomaterial Design', Journal of Macromolecular Science, Part A, 44: 9, 1041 — 1046
To link to this Article: DOI: 10.1080/10601320701424487
URL: http://dx.doi.org/10.1080/10601320701424487

Journal of Macromolecular Science ®, Part A: Pure and Applied Chemistry (2007) **44**, 1041–1046

ISSN: 1060-1325 print / 1520-5738 online
DOI: 10.1080/10601320701424487

Dedicated to the 80th Birthday of Dr. Otto Vogl, Herman F. Mark Professor Emeritus

Degradation Profile of Poly(ε-caprolactone)—the Influence of Macroscopic and Macromolecular Biomaterial Design

ANDERS HÖGLUND, MINNA HAKKARAINEN, and ANN-CHRISTINE ALBERTSSON

Department of Fibre and Polymer Technology, School of Chemical Science and Engineering, Royal Institute of Technology, Stockholm, Sweden

Received and accepted March, 2007

Macroscopic and macromolecular material design and their influence on hydrolysis mechanism of poly(ε-caprolactone) (PCL) was evaluated. Homogenous discs of linear PCL, porous scaffolds of linear PCL and crosslinked PCL networks were subjected to hydrolytic degradation for up to 364 days in 37°C and pH 7.4 phosphate buffer solution. After different hydrolysis times, mass loss and changes in molecular weight and thermal properties were determined in parallel to extraction and analysis of the formed degradation products. Size exclusion chromatography (SEC), differential scanning calorimetry (DSC) and gas chromatography-mass spectrometry (GC-MS) were used for the analyses. The results clearly demonstrated different degradation profiles and susceptibilities towards hydrolysis depending on the macroscopic and macromolecular biomaterial design.

Keywords: degradation; hydrolysis; poly(ε-caprolactone); macromolecular design

1 Introduction

An essential aspect in the field of tissue engineering when designing a biocompatible material is to adjust the degradation rate. Polymeric scaffolds serve as support and guidance to proliferation of cells and are intended to be gradually resorbed as they are replaced by the extracellular matrix of the cells. The most prominent family of materials used in tissue engineering is the aliphatic polyesters derived from cyclic monomers, e.g. lactic acid (LA), glycolic acid (GA) and ε-caprolactone (ε-CL). These polymers have been demonstrated as biocompatible in a number of applications, such as scaffold preparation (1) and drug delivery (2). PCL is also well suitable as a material for fabrication of 3D scaffolds in tissue engineering since its low melting temperature and high decomposition temperature (350°C) entails an extensive range for thermoplastic processing (3, 4).

Degradation of aliphatic polyesters *in vivo* occurs via random hydrolytic scission of ester bonds (5). However, the degradation rate of PCL is considerably slower compared to other aliphatic polyesters due to its hydrophobicity and high crystallinity. Biotic degradation of PCL has been studied extensively during the past three decades, where accordant results have demonstrated PCL to be readily biodegradable in numerous environments (6). In addition, concurrent effect of temperature and microorganisms entail faster degradation rate (7–9). *In vivo* degradation of PCL has also been investigated by several groups (5, 10, 11). However, pure abiotic hydrolysis of PCL has been studied less, probably due to the prolonged degradation time. Chen et al. compared *in vitro* degradation of PCL microparticles and PCL discs (12). He did not see any obvious effect of shape on the degradation rate. However, the PCL particles were prepared by emulsification and hence, had a smaller surface area compared to a porous structure. Otherwise, copolymerization and blending are well-known procedures to alter the mechanical properties and degradation rate of PCL.

Progress in polymer synthesis has revealed the opportunity to design novel polymers with customized properties and degradation profiles. Our group has recently reported that the release rate of degradation products from PCL copolymers is controllable by means of macromolecular design (13). We have also demonstrated the applicability of using crosslinking in combination with altered hydrophilicity in order to control degradation rate and release of degradation

Address correspondence to: Ann-Christine Albertsson, Department of Fibre and Polymer Technology, School of Chemical Science and Engineering, Royal Institute of Technology, S-100 44, Stockholm, Sweden. Tel.: +46-8-790 82 74; Fax: +46-8-10 07 75; E-mail: aila@polymer.kth.se

products (14). The aim of this study is to evaluate the effect of macroscopic and macromolecular design on biomaterial degradation profile and mechanism. Therefore, three PCL homopolymers with different macroscopic designs were synthesized: linear homogenous discs, porous structures and cross-linked networks. The hydrolytic degradation of the materials was monitored for up to 364 days.

2 Experimental

2.1 Materials

ε-caprolactone (CL) (Aldrich, Germany) was dried and subsequently distilled over CaH_2 at reduced pressure prior to use. Stannous octoate ($SnOct_2$) (Aldrich, Germany) was also distilled under reduced pressure. All reactants were stored in a glove box (Mbraun MB150B-G-I, Germany) under an inert atmosphere before use. Chloroform (Bergman-Labora, Sweden) stabilized with 2-methyl-2-butene, was dried over CaH_2 for 24 h and thereafter distilled under reduced pressure in an inert atmosphere just before use. The cyclic tin alkoxide 1,1,6,6-tetra-n-butyl-1,6-distanna-2,5,7,10-tetraoxacyclodecane was synthesized from dibutyltin oxide and 1,2-ethanediol as described in the literature (15). 2,2′-bis-(ε-caprolactone-4-yl) propane (BCP) was synthesized according to a modified approach (16) of the procedure given elsewhere (17).

2.2 Polymerization Technique

Reaction vessels were silanized and glassware and syringes were flame-dried prior to use. The synthesis of the PCL homopolymer for linear disc preparation was performed according to the literature (15). The monomer, initiator and chloroform were added to the reaction vessel under an inert atmosphere and allowed to react by ring-expansion polymerization until complete conversion. For the porous PCL, monomer, coinitiator and catalyst were weighed into a 25 mL round-bottom flask inside the glove box. The flask was equipped with a magnetic stirrer bar and subsequently sealed using a three-way valve. Polymerization was carried out by placing the flask into a thermostated oil bath at 110°C for 10 h. The polymers were precipitated in a mixture of cold hexane and methanol (95:5). PCL linear discs were prepared by dissolving the polymer in chloroform followed by solution-casting into a thin film (0.1 mm) on a glass plate. The solvent was evaporated, and the film was dried under reduced pressure for 1 week before analysis. Round polymeric discs were thereafter punched from the dried films. Porous structures were obtained using a solvent casting and salt particulate leaching technique (18). The CL network was synthesized by ring-opening polymerization of CL with BCP as crosslinking agent using $SnOct_2$ as catalyst (16). The crosslinked samples had a thickness of approximately 0.5 mm.

2.3 Hydrolysis

The different PCL polymers were subjected to hydrolytic degradation in a 37°C saline buffer with a pH of 7.4. The buffer was prepared by dissolving 45 g NaCl, 53.65 g $Na_2HPO_4 \cdot 7H_2O$ and 10.6 g NaH_2PO_4 in 4800 ml of deionized water. The mixture was stirred overnight, and thereafter pH adjusted to 7.4 by addition of 1 M NaOH and diluted to 5000 ml with deionized water. For the hydrolysis, approximately 10 mg of polymer was placed in a glass vial containing 10 ml of the saline solution and 100 μl 0.04 wt% NaN_3 solution in order to prevent microbial growth. The sample vials were sealed with septa, and subsequently put in a thermostatically controlled incubator with temperature set to 37°C and rotation to 60 rpm. Triplicate samples from each material were withdrawn from the buffer after 1, 7, 28, 91, 182, and 364 days of degradation, and analyzed.

2.4 Water Absorption and Mass Loss

The percentage mass loss after different hydrolysis times was measured after drying the samples for two weeks at reduced pressure (0.5×10^{-3} mbar) by comparing the dry weight (m_d) at a specific time with the initial weight according to Equation (1).

$$\Delta m_d = \frac{m_0 - m_d}{m_0} \times 100 \quad (1)$$

2.5 Size Exclusion Chromatography, SEC

SEC was used to determine the molecular weights of the polymers prior to and after hydrolysis. N,N-dimethylformamide (LabScan, Sweden) at a flow rate of 1.0 mL/min was used as the eluent. The injection volume was 50 μL. A Waters 717 Plus autosampler and a Waters model M-6000A solvent pump equipped with a PL-EMD 960 light scattering evaporative detector, two PLgel 10-mm mixed B columns (300 × 7.5 mm) from Polymer Laboratories, and one Ultrahydrogel linear column (300 × 7.8 mm) from Waters, connected to an IBM-compatible computer, were used. Narrow molecular-weight polystyrene standards were used for calibration. Millennium software version 3.20 was used to process the data. The number average molecular weight (M_n) was used to analyze the kinetics of the hydrolysis. A kinetic model for the chain scission of aliphatic polyesters has been derived by Pitt et al. (19). The degradation rate is given by the rate constant k in Equations (2) and (3) where $M_{n,0}$ is the original number average molecular weight.

$$\ln(M_n) = \ln(M_{n,0}) - k_2 t \quad (2)$$

$$\frac{1}{M_n} = \frac{1}{M_{n,0}} + k_3 t \quad (3)$$

Equations (2) and (3) refer to the auto-catalyzed and the non-catalyzed reaction, respectively. $\ln(M_n)$ and $1/M_n$ is plotted as a function of degradation time and a linear trend line is

adjusted to the data points. The equation which gives the best linear fit indicates the dominating mechanism. M_n was also used to determine the number of chain scissions (n) after different hydrolysis times using Equation (4)

$$n = \frac{1}{M_n} - \frac{1}{M_{n,0}} \tag{4}$$

2.6 Differential Scanning Calorimetry, DSC

A Mettler Toledo DSC 820 module operating under nitrogen atmosphere was used to measure the thermal properties of the PCL polymers. 5–10 mg of the polymer was encapsulated in a 40-μL aluminum cap without pin. Samples were heated under a nitrogen gas flow of 50 mL/min from −65 to 80°C at a rate of 10°C/min. The samples were thereafter cooled from 80 to −65°C at a rate of 10°C/min before being heated again from −65 to 80°C at a rate of 10°C/min. The melting temperatures, T_m, were noted as the maximum values of the melting peaks and the midpoint temperature of the glass transition was determined as the glass transition temperature, T_g, from the first heating scan. The approximate crystallinity of the polymers was calculated according to Equation 5:

$$w_c = \frac{\Delta H_f}{\Delta H_f^0} \times 100 \tag{5}$$

where w_c is the degree of crystallinity, ΔH_f is the heat of fusion of the sample, and ΔH_f^0 is the heat of fusion of 100% crystalline polymer. 139.5 J/g was used as value for ΔH_f^0 (20).

2.7 Solid Phase Extraction (SPE)

Solid phase extraction (SPE) was used to extract the hydrolysis products from the buffer medium. 2 ml of the phosphate buffer containing the degradation products were removed from each sample vial. 200 μl of 1 mg/ml D,L-2-hydroxyvaleric acid sodium salt (Prosynth LTD, Suffolk, UK) internal standard solution was added and pH was lowered to 1 by addition of 37% HCl. 1 ml ENV + SPE columns (Sorbent AB, Västra Frölunda, Sweden) were used in the extractions. Firstly, the columns were conditioned with 2 ml methanol and equilibrated with 2 ml acidified (pH = 1) phosphate buffer solution. The 2 ml sample portion was subsequently allowed to pass through the column, after which the retained hydrolysis products were eluted with 0.5 ml acetonitrile and finally analyzed with GC-MS.

2.8 Gas Chromatography-Mass Spectroscopy (GC-MS)

Chromatographic separation followed by mass detection was executed using a ThermoFinnigan (San José, CA, USA) GCQ GC-MS system. A Gerstel (Mülheim an der Ruhr, Germany) MPS2 autosampler was used for injecting the samples. The GC was equipped with a WCOT CP-Wax 52 CB column (30 m × 0.25 mm × 0.25 μm) from Varian (Lake Forest, CA). The column temperature was kept at 40°C for 1 min, and thereafter programmed to 250°C at 10°C/min, and subsequently, the column was held at the elevated temperature for 13 min. The injection temperature was 250°C and a splitless injection mode was used. Helium of 99.9999% purity from AGA (Stockholm, Sweden) was used as carrier gas at a constant average linear velocity of 40 cm/s controlled by the Electronic Pressure Control (EPC) of the GC. The temperatures of the transfer line and the ion source were 275°C and 180°C, respectively. A scanning range of 35–400 m/z with a scan time of 0.43 sec was used by the mass spectrometer. The peak areas were determined by integrating the Total Ion Current (TIC) using Xcalibur 1.2 software.

3 Results and Discussion

Three different polycaprolactone (PCL) homopolymers were subjected to hydrolytic degradation in phosphate buffer solution for up to 364 days. The three polymers were linear homogenous discs, porous structures and crosslinked networks and were designed to study the influence of macroscopic and macromolecular biomaterial design on PCL degradation profile. The molecular weights and thermal properties prior to hydrolytic degradation are presented in Table 1.

3.1 Degradation Products

The monomeric hydrolysis product, 6-hydroxyhexanoic acid (HHA), was extracted from the phosphate buffer and thereafter analyzed by GC-MS. Figure 1 shows the relative amount of HHA released during the degradation of the different PCL homopolymers. The largest amount of monomeric hydroxy acid was released from the PCL network, with 2.5 times more HHA detected after 364 days compared to the linear PCL. This is probably mostly due to the considerably lower degree of crystallinity for the cross-linked polymer which makes it easier for the water to migrate into the material. DSC measurements indicated a disruption in the network structure after 28 days, which coincides with the rapid increase in HHA release after 91 days. The amount of HHA released from the porous structure was practically undetectable during the first 182 days and was only about 10% of the amount released from the linear PCL discs after 364 days.

Table 1. Molecular weight and thermal properties of the PCL polymers prior to degradation

Polymer name	M_n[a] [g/mol]	PDI[a]	T_m[b] [°C]	w_c[b] [%]
Linear disc	30,000 ± 600	1.44 ± 0.01	63.3 ± 0.4	78.2 ± 0.2
Porous structure	82,000 ± 650	1.33 ± 0.02	67.0 ± 0.3	69.2 ± 2.0
Network	—	—	43.6 ± 0.5	29.3 ± 4.2

[a]Determined using DMF SEC calibrated with narrow molecular weight polystyrene standards.
[b]Determined from the first heating scan.

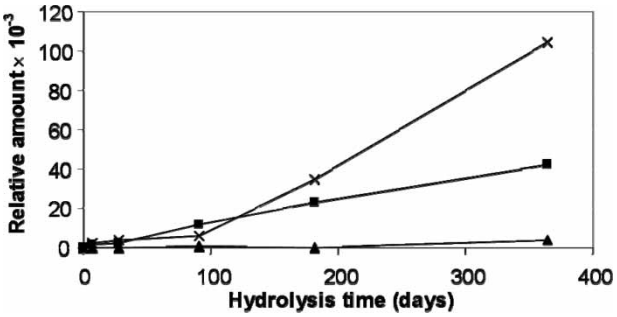

Fig. 1. Total amount of released 6-hydroxyhexanoic acid for (▲) porous structure, (■) linear disc and (×) network during the hydrolysis.

3.2 Mass Loss

The hydrolytic degradation was also followed by determining the mass loss after different hydrolysis times (Figure 2). All three PCL polymer types show similar and relatively low mass loss during the first 182 days where after their mass loss profiles diverge. The largest mass loss was observed for the network which increased from 4.5% to 16% between 182 and 364 days. In contrast, mass loss for the porous structure remains at very low levels throughout the degradation period. The linear PCL shows an intermediate mass loss profile compared to the others. The large mass loss for the network is due to the significantly lower crystallinity of the crosslinked structure as the amorphous regions are known to be more sensitive towards hydrolysis and degrade prior to crystalline regions. The large difference in mass loss between the porous structure and linear disc is probably due to both the differences in the molecular weight and the different macroscopic designs. Previous studies have shown a porosity of 91.5% for the studied porous PCL material (18). Other groups have reported that degradation rate of porous polymeric structures decrease with increasing porosity and pore sizes (21–23). It is believed that larger surface areas and thinner pore walls facilitated the diffusion of acidic degradation products and hence suppresses the auto-catalyzed hydrolysis process.

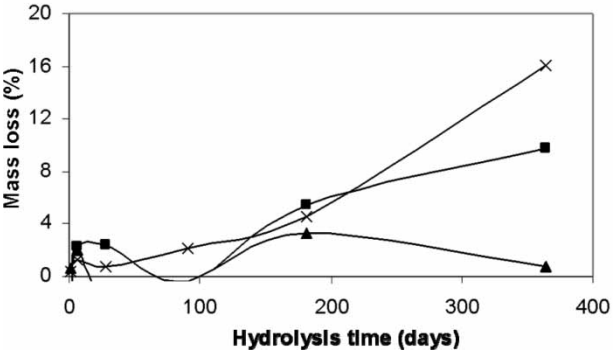

Fig. 2. Mass loss profiles for (▲) porous structure, (■) linear disc and (×) network during degradation.

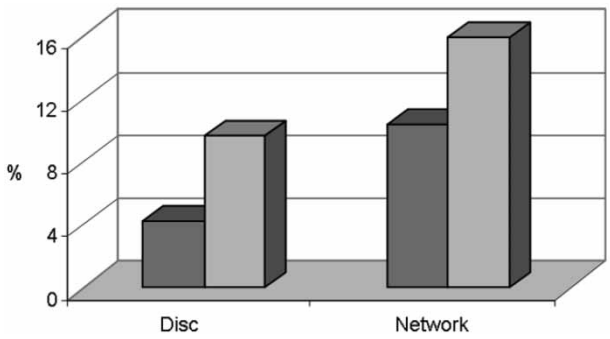

Fig. 3. Comparison of (□) mass loss and (■) relative amount of monomeric degradation products released from the linear PCL disc and PCL network after 364 days of hydrolysis.

Figure 3 compares the mass loss to the relative amount of 6-hydroxyhexanoic acid (HHA) released after 364 days of hydrolysis for linear PCL disc and network PCL. Larger amount of monomeric HHA in relation to mass loss was released from the network structure in comparison to the PCL disc. However, the largest amount of water-soluble oligomers in relation to total mass loss was released from the linear disc. Due to the crosslinked structure a larger number of chain scissions is needed for the release of water-soluble products from the network, which pushes the degradation product pattern towards the monomeric hydroxy acid. A similar trend was also observed in a previous study when comparing the hydrolysis of CL and DXO (1,5-dioxepan-2-one) copolymers (13). An equivalent comparison of the porous structure was not made due to the very low mass loss and small amount of released HHA.

3.3 Molecular Weight Changes

SEC was used to determine molecular weights and polydispersity indexes for the linear disc and porous structure after different degradation times. The network was insoluble due to its crosslinked structure and the molecular weight could therefore not be determined. The molecular weight changes were also used to evaluate the degradation kinetics. A decrease in molecular weight with increasing degradation time was observed for both materials (Figure 4). The molecular weight of the

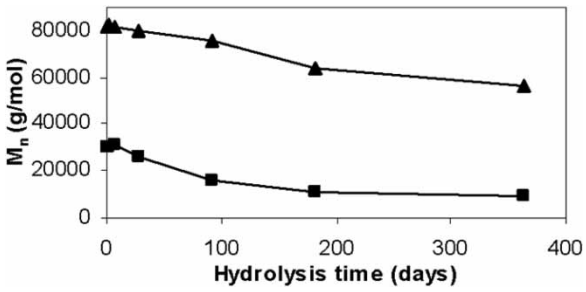

Fig. 4. Molecular weight changes for (▲) porous structure and (■) linear disc during hydrolysis.

linear PCL disc decreased from 30,000 to 9000 g/mol during the hydrolysis study. Hence, only 30% of the initial molecular weight remains after 364 days. The critical molecular weight for onset of mass loss for PCL has been demonstrated to be approximately 5000 (5). If looking at Figures 2 and 4, this corresponds rather well with our results. For the porous structure, M_n decreases from 82,000 to 56,000 g/mol during the same time period, which means 69% of the initial molecular weight remained at the end of the study. In addition, the molecular weight drops faster for the linear PCL disc and the decrease starts more or less immediately after the samples were immersed into the buffer solution. This is also illustrated in Figure 5 which shows the number of chain scissions as a function of hydrolysis time for the linear and porous structures, respectively. Fewer chain scissions occur in the porous structure compared to the linear disc. In addition, the difference increases with hydrolysis time. This also indicates a higher hydrolysis rate of the linear disc than the porous structure. This disparity could also be observed when comparing the polydispersity indexes of the different materials, Figure 6. Polydispersity index (PDI) for the porous structure is relatively constant at 1.3 during the first 91 days where after it increases slightly to 1.4. For the linear PCL disc, however, PDI increases from 1.4 to 1.7 between 28 and 182 days. This is also a consequence of the larger number of chain scissions taking place in the PCL discs. A broader distribution of chains is obtained since the chain scission process of PCL occurs randomly (5). The decrease in PDI between 182 and 364 days is probably due to the substantial mass loss observed during the same time period. M_w decreases faster than M_n between 182–364 days, and this is probably a consequence of a continuous hydrolysis of the longer chains whereas the shorter chains become soluble in the buffer solution.

The kinetics of the hydrolysis process was also studied to determine if the hydrolysis was mainly auto-catalyzed or non-catalyzed. In Figures 7a and 7b $\ln(M_n)$ and $1/M_n$ for the linear disc and porous material were plotted as a function of hydrolysis time. The expression of the catalyzed reaction is valid until the carboxylic end group concentration is decreased due to the loss of oligomers from the polymer bulk (19). As seen in Figure 7, there were no big differences

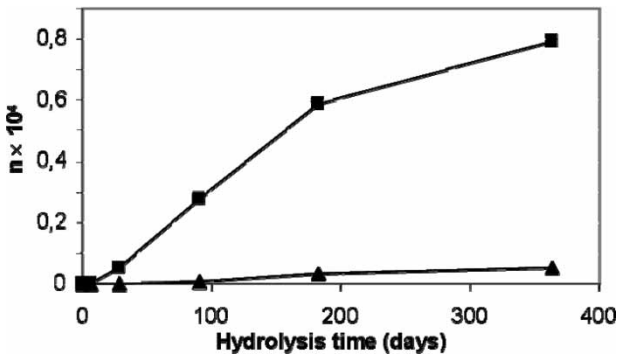

Fig. 5. Number of chain scissions (n) for (▲) porous structure and (■) linear disc during the hydrolysis.

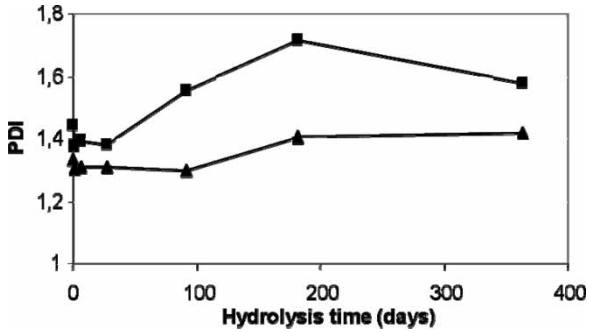

Fig. 6. Changes in Polydispersity index (PDI) for (▲) porous structure and (■) linear discs during the hydrolysis.

in the R^2 values for the two materials and auto-and non-catalyzed reactions. However, the linear discs had a R^2 value of 0.9946 for the auto-catalyzed reaction and 0.9898 for the non-catalyzed reaction. On the contrary, the corresponding values for the porous structure were 0.9929 and 0.9942. Although the differences are rather small, it still gives a vague indication of a faster and more acid-catalyzed hydrolysis for the linear disc compared to the porous structure.

3.4 Thermal Properties

Thermal properties of the PCL homopolymers before and after aging were determined by DSC. Figure 8 shows the

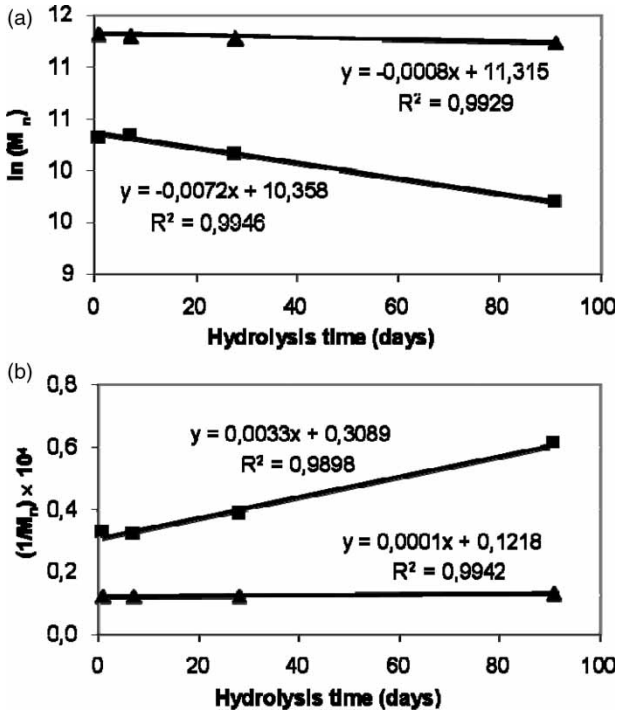

Fig. 7. (a) Degradation kinetics for (▲) porous structure and (■) linear disc during the hydrolysis described by auto-catalyzed reaction; (b) Degradation kinetics for (▲) porous structure and (■) linear disc during the hydrolysis described by non-catalyzed reaction.

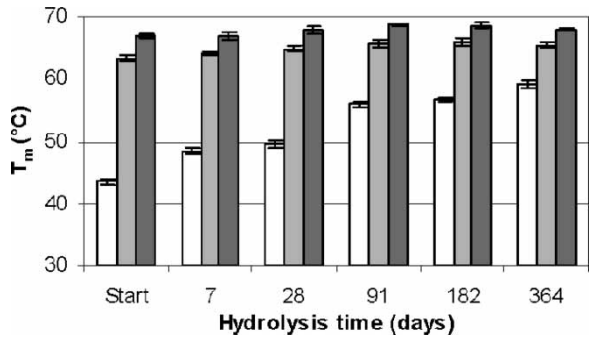

Fig. 8. Influence of the degradation time on the melting temperature for (□) network, (▣) linear disc and (■) porous structure determined from the first heating scan.

melting points (T_m) for the materials after different hydrolysis times. The melting points for the linear disc and porous structure are relatively unaffected by the hydrolysis. Only a slight increase in T_m is observed with degradation time indicating a diminutive effect of the hydrolysis on the PCL crystals. In contrast, T_m for the network increases continuously from 43.6°C to 59.1°C. In addition, the degree of crystallinity (w_c) also increases from 29.3% to 51.6% reducing the initial difference between the discs and porous structure. Network structures have been reported to have approximately 25–30% lower crystallinity than their linear analogues (24). Chain mobility is confined by the crosslinks and the incorporation of crosslinking agents further disturbs the crystallization. The increase in w_c for the network is a consequence of the faster degradation of the amorphous regions. The network structure is also disrupted during the degradation which increases the mobility of the chains and hence, their ability to crystallize. Thicker and more perfect lamellae are formed which causes the observed increase in T_m.

4 Conclusions

The degradation profile of PCL and its susceptibility towards hydrolysis were altered when the macroscopic and macromolecular structures were modified. Introduction of crosslinks shifted the degradation product patterns towards monomeric hydroxy acids, while larger amount of water soluble oligomers in comparison to mass loss was released from the linear PCL disc. The susceptibility of PCL towards hydrolysis was increased by introduction of cross-links. Crosslinking lowered the degree of crystallinity, which in turn considerably increased the hydrolysis rate. The high porosity and thin pore walls in the case of the porous structure together with higher molecular weight implied a pronounced resistance towards hydrolysis compared to both linear PCL discs and PCL network.

5 Acknowledgements

The authors gratefully acknowledge The Swedish Foundation for Strategic Research (Grant no. A302:139) for their financial support of this work.

6 References

1. Agrawal, C.M. and Ray, R.B. (2001) *J. Biomed. Mater. Res.*, **55**(**2**), 141–150.
2. Edlund, U. and Albertsson, A.-C. (2002) *Adv. Polym. Sci.*, **157**, 67–112.
3. Hutmacher, D.W. (2000) *Biomaterials*, **21**(**24**), 2529–2543.
4. Hutmacher, D.W., Schantz, T., Zein, I., Ng, K.W., Teoh, S.H. and Tan, K.C. (2001) *J. Biomed. Mater. Res.*, **55**(**2**), 203–216.
5. Pitt, C.G., Chasalow, F.I., Hibionada, Y.M., Klimas, D.M. and Schindler, A. (1981) *J. Appl. Polym. Sci.*, **26**(**11**), 3779–3787.
6. Hakkarainen, M. (2002) *Adv. Polym. Sci.*, **157**, 113–138.
7. Albertsson, A.-C., Renstad, R., Erlandsson, B., Eldsater, C. and Karlsson, S. (1998) *J. Appl. Polym. Sci.*, **70**(**1**), 61–74.
8. Eldsater, C., Erlandsson, B., Renstad, R., Albertsson, A.-C. and Karlsson, S. (1999) *Polymer*, **41**(**4**), 1297–1304.
9. Hakkarainen, M. and Albertsson, A.-C. (2002) *Macromol. Chem. Phys.*, **203**(**10**/**11**), 1357–1363.
10. Sung, H.-J., Meredith, C., Johnson, C. and Galis, Z.S. (2004) *Biomaterials*, **25**(**26**), 5735–5742.
11. Sun, H., Mei, L., Song, C., Cui, X. and Wang, P. (2006) *Biomaterials*, **27**(**9**), 1735–1740.
12. Chen, D.R., Bei, J.Z. and Wang, S.G. (2000) *Polym. Degrad. Stab.*, **67**(**3**), 455–459.
13. Hakkarainen, M., Höglund, A., Odelius, K. and Albertsson, A.-C. (2007) *J. Am. Chem. Soc.*, **129**(**19**), 6308–6312.
14. Höglund, A., Odelius, K., Hakkarainen, M. and Albertsson, A.-C. (2007) *Biomacromolecules.*, **8**(**7**). Available online.
15. Stridsberg, K. and Albertsson, A.-C. (1999) *J. Polym. Sci., Part A: Polym. Chem.*, **37**(**16**), 3407–3417.
16. Andronova, N., Srivastava, R.K. and Albertsson, A.-C. (2005) *Polymer*, **46**(**18**), 6746–6755.
17. Palmgren, R., Karlsson, S. and Albertsson, A.-C. (1997) *J. Polym. Sci., Part A: Polym. Chem.*, **35**(**9**), 1635–1649.
18. Odelius, K., Plikk, P. and Albertsson, A.-C. (2005) *Biomacromolecules*, **6**(**5**), 2718–2725.
19. Pitt, C.G. and Gu, Z.W. (1987) *J. Controlled Release*, **4**(**4**), 283–292.
20. Crescenzi, V., Manzini, G., Calzolari, G. and Borri, C. (1972) *Eur. Polym. J.*, **8**(**3**), 449–463.
21. Agrawal, C.M., McKinney, J.S., Lanctot, D. and Athanasiou, K.A. (2000) *Biomaterials*, **21**(**23**), 2443–2452.
22. van Tienen, T.G., Heijkants, R.G.J.C., Buma, P., de Groot, J.H., Pennings, A.J. and Veth, R.P.H. (2002) *Biomaterials*, **23**(**8**), 1731–1738.
23. Wu, L. and Ding, J. (2005) *J. Biomed. Mater. Res.*, **75A**(**4**), 767–777.
24. Albertsson, A.-C. and Gruvegaard, M. (1995) *Polymer*, **36**(**5**), 1009–1016.